

Accepted Manuscript

Journal of the Geological Society

Thrust-related metamorphism in Carboniferous slates of southern Patagonia (South America): The fate of forearc successions

Rodrigo Suárez, Pablo González, Sebastián Oriolo, Martín Parada, Miguel E. Ramos, Matías C. Ghiglione, Claudia Zaffarana, Juan Albano & Juan J. Ponce

DOI: <https://doi.org/10.1144/jgs2023-173>

To access the most recent version of this article, please click the DOI URL in the line above. When citing this article please include the above DOI.

This article is part of the Ophiolites, melanges and blueschists collection available at: <https://www.lyellcollection.org/topic/collections/ophiolites-melanges-and-blueschists>

Received 8 October 2023

Revised 11 February 2024

Accepted 17 March 2024

© 2024 The Author(s). Published by The Geological Society of London. All rights reserved. For permissions: <http://www.geolsoc.org.uk/permissions>. Publishing disclaimer: www.geolsoc.org.uk/pub_ethics

Supplementary material at <https://doi.org/10.6084/m9.figshare.c.7160849>

Manuscript version: Accepted Manuscript

This is a PDF of an unedited manuscript that has been accepted for publication. The manuscript will undergo copyediting, typesetting and correction before it is published in its final form. Please note that during the production process errors may be discovered which could affect the content, and all legal disclaimers that apply to the journal pertain.

Although reasonable efforts have been made to obtain all necessary permissions from third parties to include their copyrighted content within this article, their full citation and copyright line may not be present in this Accepted Manuscript version. Before using any content from this article, please refer to the Version of Record once published for full citation and copyright details, as permissions may be required.

Thrust-related metamorphism in Carboniferous slates of southern Patagonia (South America): The fate of forearc successions

Rodrigo Suárez^{*1,2}, Pablo González^{2,3,4}, Sebastián Oriolo⁵, Martín Parada¹, Miguel E. Ramos⁶, Matías C. Ghiglione⁶, Claudia Zaffarana^{1,2}, Juan Albano⁶, Juan J. Ponce^{2,3,4}

¹*Instituto de Investigación en Paleobiología y Geología (IIPG; UNRN–CONICET).*

²*Universidad Nacional Río Negro (UNRN), Sede Alto Valle y Valle Medio, General Roca.*

³*Consejo Nacional de Investigaciones Científicas y Técnicas (CONICET).*

⁴*Servicio Geológico Minero Argentino (SEGEMAR), Río Negro, Argentina.*

⁵*Instituto de Geociencias Básicas, Aplicadas y Ambientales de Buenos Aires (IGEBA; UBA – CONICET).*

⁶*Instituto de Estudios Andinos “Don Pablo Groeber” (IDEAN; UBA–CONICET).*

**Corresponding author. Dr. Rodrigo Javier Suárez. Instituto de Investigación en Palaeobiología y Geología (UNRN – CONICET), Av. General Roca 1242 (General Roca, Río Negro, Argentina). Personal e-mail: rodrigo_s_37@hotmail.com; Institutional e-mail: rjsuarez@unrn.edu.ar;*

Abstract. The Devonian to early Carboniferous western margin of Patagonia (South America) includes a NW-SE-trending magmatic arc associated with a palaeo NE-dipping subduction zone. Along the Andean region of southern Patagonia, the Eastern Andean Metamorphic Complex (EAMC) developed in a forearc position, consisting of a succession of very low- to low-grade metaturbidite-metabasic rocks emplaced from the Devonian to Carboniferous periods. There are significant uncertainties surrounding this metamorphic complex, mainly related to the tectonosedimentary setting of the basin and subsequent conditions of deformation and metamorphism, which hinder our understanding of the orogenic architecture. To reveal the link between tectonics and metamorphism, we conducted a structural analysis and sampled metapelites to measure illite crystallinity along a regional structural cross-section in the EAMC. Our analysis reveals broadly Lower to Upper Anchizonal metamorphism which is roughly synchronous with deformation along northward-verging thrusts. These findings support the development of a forearc hyperextended basin that was subsequently closed during the Gondwanide orogeny (late Paleozoic), a model that reconciles previous proposals suggesting passive margin vs. back-arc basin models. This closure led to the emplacement of suprasubduction zone ophiolites and turbidites over the continent through landward migration of brittle-ductile reverse shear zones.

Supplementary Material. Measurements of Kübler Index are available at'.

Providing quantitative constraints on very low- to low-grade metamorphic conditions is one of the challenges of metamorphic petrology. While a methodology to assess medium- to high-grade metamorphic processes is well-developed (e.g. modelling of phase equilibrium), such tools are hard to apply in very low- to low-temperature conditions due to the presence of protolith relicts, which hamper the possibility to determine the effective bulk composition (Lanari and Engi 2017). Nowadays, assessing the crystallographic transformation of layer silicate minerals (*i.e.* smectite-corrensite-chlorite and smectite-illite-muscovite) is still the best approach to obtain insights on these metamorphic conditions and its link with large-scale tectonometamorphic processes (Robinson and Merriman 1999; Verdecchia *et al.* 2021; Hueck *et al.* 2022).

Two of the most extensively studied crystallochemical indexes for characterization of very low- to low-grade metapelitic successions are the Kübler Index (KI) (Kübler 1968) for white micas and the Arkai Index for chlorites (AI) (Arkai 1991), both based on XRD (X-ray diffraction) analysis (see review in Kübler and Jaboyedoff 2000). The crystallinity of layer silicates is translated to metamorphic conditions and, when complemented with structural studies, powerful insights on the orogenic anatomy and strain-related processes can be obtained based on patterns of crystallinity values (von Gosen *et al.* 1991; Merriman and Frey 1999; Robinson and Bevins 1999; Valín *et al.* 2016; Süssenberger *et al.* 2018; Hueck *et al.* 2020). For example, burial patterns (e.g. Robinson and Bevins 1986; Roberts 1991, 1996), relative timing between deformation and metamorphism (e.g. Jamienson *et al.* 1996; Warr *et al.* 1996; Valín *et al.* 2016; Hueck *et al.* 2020), and orogenic anatomy (e.g. von Gosen *et al.* 1991; Süssenberger *et al.* 2018), can be disentangled by deciphering the relationship between very low- to low-grade metamorphism and tectonics (see Merriman and Frey 1999).

Along the Cordilleran region of southern Patagonia in South America (figs. 1, 2), a succession of very low- to low-grade metasedimentary rocks deposited in Devonian-Carboniferous times crops out, which is grouped under the Eastern Andean

Metamorphic Complex (EAMC) (Fig. 2) (see Hervé *et al.* 2008). Around this metamorphic complex, there is an ongoing debate on the tectonic setting of sedimentation, and subsequent deformation and metamorphism (e.g. Augustsson *et al.* 2006; Rojo *et al.* 2021; Suárez *et al.* 2021). Classically, a passive margin (i.e. no active subduction) was interpreted during deposition, as suggested by provenance analysis, which identified a rich-quartz “mature” protolith with provenance from Gondwana inland (Hervé *et al.* 2003; Lacassie, 2003; Augustsson *et al.* 2006; Augustsson and Bahlburg 2008). Under this vision, deformation and metamorphism took place in the accretionary prism in a framework of east-dipping renewed subduction during late Palaeozoic times (e.g. Augustsson *et al.* 2006). New evidence supplied during the last years challenges this classic vision and provide a new perspective to address this metamorphic complex. In this regard, Rojo *et al.* (2020, 2021) proposed the existence of a back-arc basin based on geochemistry and isotope data in mafic-ultramafic rocks –including serpentinites-. In any case, the closure of the oceanic basin could be related to the Gondwanide orogeny in a setting of fold-thrust belt, as depicted by Suárez *et al.* (2021).

A weak point in the above stated proposals is the lack of estimation of metamorphic conditions and its relationship with the structural evolution. Hervé *et al.* (1999) were the first in noting that the tectonic setting of metamorphism in the EAMC presents some differences regarding the classic accretionary complexes, as those identified along the Chilean coast. In this way, they estimated a low to intermediate P-T gradient in meta-pillow lavas. Then, Ramírez-Sánchez *et al.* (2005) defined P-T metamorphic conditions of 4.0 ± 1.2 kbar and 390-320 °C in metapelites, indicating a rather typical Barrovian gradient.

In this study, we apply XRD analysis in metapelites in order to provide constraints of metamorphic conditions based on Illite cristallinity, which are also integrated with structural studies. To fill the gap of information south of the sampling sites of Ramírez-

Sanchez *et al.* (2005) (see Fig. 2), we focused on the sector of the EAMC located between 48.5-49.5 °S in the South Patagonian Andes (Fig. 2). Our findings provide new evidence to evaluate the orogenic architecture of the EAMC and its relationship with Middle-to-late Palaeozoic tectonics of southern Patagonia-Antarctic Peninsula.

Geological framework

Middle to late Palaeozoic tectonics of southern Patagonia. The southern Patagonian region comprises the South Patagonian Andes along the Andean Cordillera, the Deseado Massif in the extra-Andean region, and in the south, the buried basement of Tierra del Fuego (Fig. 1).

In pre-Andean times, the southern Patagonian region evolved in a framework of northeast-dipping subduction, which produces an *in-situ* southwestward crustal growth (e.g. Suárez *et al.* 2019). Based on kinematic plate reconstruction (Riley *et al.* 2023), the Antarctic Peninsula terrane might have evolved attached to the western margin of southern Patagonia (Fig. 1). In the aforementioned tectonic context, a NW-SE-trending magmatic belt crossing the entire Patagonia from the Deseado Massif to the North Patagonian Andes was active (Fig. 1) (Pankhurst *et al.* 2003; Renda *et al.* 2019; Rapela *et al.* 2021; Serra Varela *et al.* 2020; Ballivián Justiniano *et al.* 2023; Oriolo *et al.* 2023), the *Western Magmatic Belt* (Ramos 2008).

Silurian-early Carboniferous granitoids with arc-related geochemical signature in the Deseado Massif yield crystallization ages of 422-346 Ma (Fig. 1) (e.g. Pankhurst *et al.* 2003; Guido *et al.* 2004, 2005; De Barrio *et al.* 2023; Ballivián Justiniano *et al.* 2023). In the western region of the Deseado Massif, successions of meta-turbidites interbedded with calc-silicate and meta-basic rocks, identified both by surface and borehole data, record a Devonian trench-forearc system (Moreira *et al.* 2013; Permuy-Vidal *et al.* 2014). These ages partially overlap with the development of the EAMC (Devonian-Carboniferous) along the South Patagonian Andes (see Suárez *et al.* 2019).

Lithology and stratigraphy of the EAMC. In the Andean region of southern Patagonia (i.e. the South Patagonian Andes) crops out the Eastern Andean Metamorphic Complex (EAMC) (figs. 1, 2) (*sensu* Hervé *et al.* 2008), which comprises metapelitic and metasedimentary rocks and subordinate marbles, serpentinites, and metabasic –mostly meta-pillow lava- rocks (Riccardi 1971; Hervé *et al.* 1999, 2003; Augustsson *et al.* 2006; Rojo *et al.* 2020, 2021). Exceptionally, successions of metamafic rocks are well exposed in the La Carmela Peninsula (50 km west of the study area) and the El Leones Valley (around the General Carrera Lake). The meta-pillow lavas in the La Carmela Peninsula are interbedded with metapelitic rocks, whereas (meta)mafic-ultramafic rocks are thrust onto the metasedimentary succession in the El Leones Valley. In both sectors, the metabasic rocks belong to the tholeiitic sub-series. MORB-normalized multi-element diagrams exhibit an almost flat pattern of HFSE and Ta-Nb depletion for the LILE. Mostly, these rocks plot in the field of N-MORB, which could include tectonic settings of basalt emplacement such as back-arc (BAAB) and forearc (FAB) basins (see Rojo *et al.* 2020, 2021). In the case of the Leones Valley, the succession is completed by serpentinites intruded by granitoid rocks (the Leones plutón) of calc-alkaline signature. The age of the Leones Pluton was constrained at 307 ± 10 Ma based on a K–Ar muscovite age (De La Cruz and Suárez, 2006). This succession was interpreted as an accreted fragment of upper oceanic crust intruded by near-trench magmatism (Rojo *et al.* 2020). U–Pb maximum depositional ages and provenance analysis indicates that this metamorphic complex comprises an older, northeastern belt (EAMCn) (Fig. 2) of Devonian-Carboniferous age, and a younger succession of Permian-Triassic age located in a southwest belt (EAMCs) (see Hervé *et al.* 2003; Augustsson *et al.* 2006; Augustsson and Balhburg 2008).

Several subunits have been proposed for the EAMCn: the Staines Complex, the Lago General Carrera Unit, the Río Lácteo Formation, the Cochrane Unit, and the Bahía de la Lancha Formation (see Hervé *et al.* 2008 and references therein). However, the distinction is based on geographical location and their stratigraphical relationships are

unclear. U-Pb maximum depositional ages yielded youngest peaks at 383, 362, 347, 323 and 322 Ma (Fig. 2) (Hervé *et al.* 2003; Augustsson *et al.* 2006; Malkowski *et al.* 2016; Rojo *et al.* 2021). In particular, Early Pennsylvanian maximum depositional ages obtained both in the Cerro Polo (Malkowski *et al.* 2016) and the Lancha Bay (Augustsson *et al.* 2006) (Fig. 2), in line with both preliminary palinological studies (Shell C.A.P.S.A. 1965) and the glacial record (Poire *et al.* 1999), point to a Carboniferous age (Pennsylvanian?) for the Bahía de la Lancha Formation.

Basin nature, deformation and metamorphism in the EAMCn. There is an ongoing discussion regarding the depositional environment of the EAMCn, which has been alternatively assigned to a passive vs active margin (cf. Augustsson and Bahlburg 2003). Traditionally, the EAMCn was interpreted as deposited in a passive margin (Hervé *et al.* 2003; Lacassie 2003; Augustsson *et al.* 2006) and then deformed into an accretionary prism during east-dipping renewed subduction (Forsythe 1982; Augustsson *et al.* 2006). However, this classical model has been challenged in the last years (e.g. Rojo *et al.* 2020, 2021; Suárez *et al.* 2021). Based on geochemistry of meta-pillow lava, serpentinites, metamafic and granitoid rocks, some authors argue in favour to the opening of a back-arc basin in Late Devonian times (Rojo *et al.* 2020, 2021), which was then deformed as a fold-thrust belt during the Gondwanide orogeny (e.g. Suárez *et al.* 2021).

P-T estimations on metamorphic conditions and detailed structural studies are scarce in the EAMCn (see Hervé *et al.* 2008). Hervé *et al.* (1999) reported values of 360 °C and 2-3 Kbar for meta-pillow lavas of the La Florida Peninsula (O'Higgins-San Martín Lake), based on geothermometry and geobarometry in chlorite and white mica, respectively. Ramírez-Sánchez *et al.* (2005) provided an extensive database between 47-48° S to evaluate the metamorphic conditions in metapelites of the EAMC. Based on Kf, they found that rocks of the EAMC belong mostly to the Epizone with metamorphic conditions of 4.0 ± 1.2 kbar and 390-320 °C. Regarding the structural fabric, a main NW-SE-trending foliation is described between the General Carrera-

Buenos Aires and Belgrano lakes (Yoshida 1981; Giacosa 1987; Bell and Suárez 2000; Rojo *et al.* 2020; Suárez *et al.* 2021). In particular, around the General Carrera Lake, Rojo *et al.* (2020) mapped a thrust with northeast vergence, which juxtaposes the mafic-ultramafic rocks onto the metasedimentary succession. In the Belgrano Lake, folds display NE vergence (e.g. Giacosa 1987), whereas N-vergence is inferred for a thrust system between the Viedma and San Martín (Giacosa and Márquez 2002; Giacosa *et al.* 2012; Suárez *et al.* 2021).

Methodology

Field work and sampling strategy. Field work was focused on a segment of the South Patagonian Andes between 48.5° and 49.5° S (Fig. 2). In this sector, the Bahía de la Lancha Formation crops out, as part of the EAMCn (cf. Calderón *et al.* 2016). Tectonic structures were grouped following the concept of *stage of structural development*, instead of deformation phase, as classically treated in the literature (see discussion in Fossen *et al.* 2019). We follow this line because the definition of deformation phase/s is interpretative rather than descriptive. Indeed, it requires the evaluation of several pieces of evidence including both field and analytical data (Fossen *et al.* 2019; Fossen 2020; Oriolo *et al.* 2022), which are then evaluated in the discussion.

Merriman and Frey (1999) suggested strategies for field sampling in metapelitic terrains, in order to perform analytical techniques. In particular, they proposed that utilizing structural cross-sections with the crystallinity of layer silicates is an efficient approach to illustrate the relationship between tectonics and very low- to low-grade metamorphism (see also Hueck *et al.* 2022). Following this approach, we collect metapelite samples (n=15) along a regional structural cross-section - previously carried out by Suárez *et al.* (2021) - to measure illite cristalinity using XRD (X-ray diffraction)

(Fig. 3, Table 1). Additionally, further samples were collected in adjacent areas to provide a more regional comprehension (Fig. 2, Table 1).

Analysis of X-ray powder, mineral identification, and illite cristallinity. The X-ray diffraction analysis were undertaken at INGEIS (UBA-CONICET), following the classical procedure. The analysis was carried out in both whole-rock and oriented (<2 µm) preparations with a Bruker D2 Phaser diffractometer. Measurement conditions included Cu radiation and Ni filter, with operation at 30 kv and 10mA. The mounts were scanned with a step size of 0.05°2θ, and time/step of 1 s.

The qualitative identification of clay mineral phases was determined following Moore and Reynolds (1997). Subsequently, to provide constraints on the metamorphic grade of metapelites, the Kübler index ($KI_{K\bar{u}}$) was measured using the (001) illite peak located between 7.5 and 10 Δ°2θ in both Air dry and Ethylene Glycol profiles. In this way, the full width at half maximum (FWHM) of the (001) illite basal reflection is measured (e.g. Warr 2018). Then, $KI_{K\bar{u}}$ values were calibrated to fit with the CIS (*Crystallinity Index Standard*) scale (Warr and Rice 1994; Warr and Ferreiro Mählmann 2015) by employing the standard regression equation (see more in Supplementary Material):

$$KI_{CIS} = 1.74 \times (KI_{K\bar{u}} 'INGEIS lab') - 0.0153 \quad (1)$$

Results

Geological mapping and structural analysis. The geological and structural characterization of the EAMCn, particularly of the Bahía de la Lancha Formation was partially presented by Giacosa *et al.* (2012) and Suárez *et al.* (2021). Therefore, an integrated description of both previous (Suárez *et al.* 2021) and new geological-structural data is presented below, in order to provide a framework for metamorphic constraints. It should be noted that rocks are best exposed in the eastern shore of the

San Martín Lake (i.e. the La Lancha Bay), whereas isolated outcrops at the Cerro Polo are significantly covered by the forest. For this reason, the structural description is focused on the La Lancha Bay (Fig. 4).

The Bahía de la Lancha Formation presents a first set of structures affecting the sedimentary fabric S_0 , comprising ~E-W-trending thrusts (T) and axial plane slaty cleavage (S_{sc}) of strike E-W to NE-SW. The associated F_1 folds are dispersed, but the fold axis mostly plunging to the SW with low-to-moderate angle (10-45°) (figs. 4, 5, 6). The slaty cleavage is only observed in the metapelitic layers (Fig. 6), whereas it is absent in metasandstones. Usually, the metapelitic rocks develop pencil cleavage by the intersection between the planes S_0 - S_{sc} (figs. 6, 7). Both field and regional observations, including the angular relationship between axial plane cleavage (S_{sc}) and protolith beds (S_0), indicate a mostly tight geometry of F_1 folds (Fig. 4). The above stated structures are overprinted by a younger stage of structural development, which is mainly characterized by open folds with inclined to vertical fold axes plunging to the NW (F_2) (Fig. 4).

The early stage of structures is the most intense in the study area. Under the microscope, the slaty cleavage is defined by Wm and subordinate Chl. It should be noted that the style of deformation of this first stage appears to switch from recumbent folds related to the low-angle reverse, Polo shear zone, in the Cerro Polo, to tight folds related to inclined reverse shear zones, which conforms the La Lila duplex system (Fig. 3).

Mineralogical composition and crystallographic index. Location of samples and structural position is exhibited in Table 1, and also in the regional map of Figure 2 and the regional, structural cross-section of Figure 3.

Samples of metapelitic rocks exhibit similar refraction peaks, which indicate a ubiquitous mineralogy of $Qz + Fsp + Wm + Chl \pm Kln$. Only sample BL-04 lacks in

chlorite, and the clay mineralogy is almost exclusively conformed by illite. It should be noted that this sample is a cataclastic rock taken from an reverse shear zone (Fig. 6).

The values of illite cristallinity and further aspects of the metasedimentary rocks are presented in Table 2 (see more in Supplementary Material). Kl_{CIS} values vary from 0.60 to 0.34, mainly in the range 0.45-0.35, which indicates that metamorphism took place in the transition between Lower-to-Upper Anchizone (following boundaries of Warr and Ferreiro Mählmann 2015). Kl_{CIS} values along the Cerro Polo are quite homogeneous ranging from 0.45 to 0.39 (Lower-to-Upper Anchizone), without significant differences between samples located in hanging wall (PO-01, PO-02, and PO-03) and footwall (PO-04 and PO-05). In the La Lancha Bay, the values are more variable from 0.60 to 0.37 (Upper Diagenetic zone to Upper Anchizone). While samples located in the hanging wall (BL-04, BL-05, BL-07, and BL-08) present values from 0.60 to 0.39 (Upper Diagenetic zone to Upper Anchizone), the values of samples located in the footwall (BL-01, BL-02, BL-03, and BL-06) are slightly more uniform ranging from 0.51 to 0.37 (Lower to Upper Anchizone). Exceptionally, sample BL-04 reaches the highest value at 0.60 (Upper Diagenetic zone), which is a cataclastic rock with S-C fabric (Fig. 6). Then, samples of the Cancha Rayada Peninsula (CR-01 and CR-02) yield identical values of 0.36 and 0.34 (Upper Anchizone).

Discussion

Linking very low-grade metamorphism with thrusting in the Bahía de la Lancha Formation. Fold superimposition relationships between the different stages of deformation identified in the Bahía de la Lancha Formation allow reconstructing the structural evolution. During an early stage of structural development, N-vergent thrusting produced tight folds and incipient axial plane, slaty cleavage. Then, the former set of tectonic structures was overprinted by open folds (see also Giacosa and Márquez 2002; Giacosa *et al.* 2012; Suárez *et al.* 2021). Stereoplots diagrams reveal

dispersion in the plunging of F_1 fold axes between the two sectors analyzed in this study (see Fig. 3). Part of the fold dispersion could be attributed to the strain induced by the superimposition of F_2 folds. Likewise, the variation in the plunging of fold axes between Polo Hill and La Lancha Bay could be partially attributed to the effect of Andean deformation on the basement blocks. Although the Andean deformation is beyond the scope of this study, it's noted that the rocks of Polo Hill are situated in a more interior position within the Andean fold-thrust belt compared to La Lancha Bay (e.g. Giacosa et al., 2012; Ghiglione et al. 2019), which could have resulted in greater shortening, tilting, and rotation, during the emplacement of Andean thrusts. In particular, this is verified by a paleomagnetic study conducted by Iglesia Llanos et al. (2003), which suggests approximately 60° of counter-clockwise rotation around vertical axes in the innermost region of the Andean fold-thrust belt, compared to $30\text{-}40^\circ$ in the outer region.

XRD analysis demonstrates the presence of illite and chlorite as main metamorphic minerals (Fig. 7), which is in agreement with preliminary reports of Poire et al. (1999). They noted that the metapelitic rocks in the clay fraction are mostly constituted by illite (70 %) and subordinate chlorite (30 %). Based on values of K_{ICIS} , we noted variations from 0.60 to 0.34 with average value between 0.45 and 0.35, indicating metamorphism in the transition between Lower-to-Upper Anchizone conditions. Taking into account the correlation between metapelitic zones and temperature proposed by Warr (2018), the Lower-to-Upper Anchizone boundary may be equivalent to temperatures around of $\sim 250^\circ\text{C}$. In this way, the thrusting emplacement and metamorphism would have taken place at a depth of ca. 10 km, based on the geothermal gradient of $25^\circ\text{C}/\text{km}$ proposed by Hervé et al. (1999) for rocks exposed ~ 40 km to the northwest (the Pescado Bay in Fig. 8). This is also in line with the presence of brittle-ductile shear zones and mineral associations including $Wm + Chl$.

Regarding the connection between metamorphism and tectonics, the Bahía de la Lancha Formation does not exhibit a clear trend in increasing/decreasing cristallinity values along the regional structural cross-section. Likewise, there is no systematic variation between hanging wall and footwall samples (i.e. Polo and La Lila structural domains). Only along the La Lila duplex system, there seems to be lower values in the hanging wall, which could be related to the load by thrusting emplacement. Consequently, available evidence supports previous proposals based on field and petrographic characterizations (e.g. Giacosa *et al.* 2012; Suárez *et al.* 2021), which suggested that very low-grade metamorphism is mostly contemporaneous with thrusting and the development of axial plane slaty cleavage defined by Wm + Chl. In this context, the development of a fold-thrust belt in the Bahía de la Lancha is well-documented by coupled structural and XRD data, indicating progressive deformation related to exhumation and strain localization along brittle-ductile shear zones.

Pattern of regional metamorphism in the EAMCn: Insights into orogenic architecture. In addition to the ability of illite cristallinity for revealing metamorphic conditions, further tectonic insights emerge when linking the cristallinity patterns with the structural style of metapelitic terrains. Merriman and Frey (1999) proposed several criteria for identifying tectonic settings where occurs the metamorphism based on very low-grade metamorphic trends. Within basins, the burial pattern is recognized as a trend where cristallinity increases with the age of strata (e.g. Coombs 1961; Robinson and Bevins 1989). Fossil accretionary prisms display a landward-dipping stack of thrusts (Sample and Moore 1987; Willner *et al.* 2004), where frontally accreted, younger strata are located closer to the trench (see Merriman and Roberts 1995). Typically, this environment presents high P/low T gradient of metamorphism (e.g. Willner *et al.* 2004). In contrast, foreland settings document thrusting coeval with metamorphism, showing lower values of illite cristallinity toward the hinterland zone (von Gosen *et al.* 1991; Süssenberger *et al.* 2018).

Classical interpretations of the EAMCn suggested that the clastic protolith was deposited in a passive margin during the Late Devonian to the early Carboniferous periods (Hervé *et al.* 2003; Augustsson *et al.* 2006; see also discussion in Augustsson and Bahlburg 2003). Then, the EAMCn was incorporated into the Late Palaeozoic accretionary prism (see Forsythe 1982; Hervé *et al.* 2003) when subduction initiated in the late Paleozoic (Augustsson *et al.* 2006). According to this perspective, a trend of increasing metamorphic grade toward the trench would theoretically be expected (cf. Merriman and Roberts 1995). By employing as a reference the Devonian-Carboniferous arc magmatism located in the Deseado Massif (Western Magmatic belt, see Fig. 1), we normalized the sample locations based on the "present-day horizontal distance to the palaeo-arc magmatism" (data from Ramírez-Sánchez *et al.* 2005 and this study) (figs. 8, 9). As a result, it is not revealed a similar trend of metamorphism for the entire set of samples compared to what is theoretically expected for accretionary prisms, namely, metamorphic conditions decrease as we move away from the trench (Fig. 9). Likewise, geothermal gradients of metamorphism obtained by Hervé *et al.* (1999) and Ramírez-Sánchez *et al.* (2005) are hotter than expected for prisms: 360 °C and 2-3 kbar (low-to-intermediate P/T), and 4.0 ± 1.2 kbar and 390-320 °C (intermediate P/T) (Fig. 8), respectively. In structural terms, the stacking pattern of thrusts in the Bahía de la Lancha Formation displays an inland vergence, which is opposite to the synthetic development of the accretionary wedge (e.g. Sample and Moore 1987). Alternatively, the structure of the Bahía de la Lancha Formation could be interpreted as a backthrust system, a possible alternative hypothesis. However, in northern regions of the EAMCn, around the Belgrano and General Carrera-Buenos Aires lakes, a landward vergence of fold and thrust has also been described (Giacosa 1987; Rojo *et al.* 2020), indicating that N-to-NE-vergence would be the main sense of tectonic transport of this deformation stage. Then, the development of a passive margin opening towards the proto-Pacific Ocean seems unlikely on a regional scale given the widespread occurrence of Devonian subduction-related magmatism crossing the entire

Patagonia (Pankhurst *et al.* 2003; Rapela *et al.* 2021; Oriolo *et al.* 2023), even at 48 °S (e.g. Ballivián Justiniano *et al.* 2023). Therefore, the integration of available data suggests exploring alternative models in order to explain the tectonic evolution of the EAMCn.

In recent years, a new line of investigation has emerged (see Rojo *et al.* 2020, 2021), suggesting that the EAMCn developed within the context of a back-arc basin situated between the Antarctic Peninsula and the Deseado Massif. In this scenario, the metamorphism and deformation of the EAMCn occurred during the closure of the back-arc basin (e.g. Rojo *et al.* 2021). Following this line of reasoning, we can examine Mesozoic Andean-type back-arc basins in order to gain further insights, such as the Rocas Verdes Basin (e.g. Klepeis *et al.* 2010; Calderón *et al.* 2012; Torres-Carbonel *et al.* 2020; Muller *et al.* 2020; Gallardo Jara *et al.* 2022). Several studies in the Rocas Verdes Basin have demonstrated that, as the back-arc basin closes and the ophiolitic complex is obducted, thrusting propagates inland, leading to the conformation of a retroarc, fold-thrust belt (Calderón *et al.* 2012; Muller *et al.* 2020). While this process helps us to reconcile the tectonic evolution of the Bahía de la Lancha Formation within the mid-to-late Palaeozoic tectonic context of southern Patagonia (see Calderón *et al.* 2016; Suárez *et al.* 2019; Riley *et al.* 2023), the scarcity of Devonian magmatism in the Antarctic Peninsula (only the Target Hill orthogneiss at 397-393 Ma by Millar *et al.* 2002) conspires against this model.

Regarding metamorphism, the geothermal gradients of the EAMCn are more similar to those estimated for closure of back-arc basins than for accretionary prisms (Fig. 7). Nevertheless, the weak point of this model is to explain the trend of metamorphism identified through illite crystallinity, which exhibit lower-grade rocks thrust over higher-grade rocks (figs. 8, 9). In other fossil foreland settings, such as the Sierra de la Ventana fold-thrust belt or the Meso-Cenozoic Magallanes fold-thrust belt, metamorphic conditions increase towards the hinterland (e.g. Von Gozen *et al.* 1991;

Süssenberger *et al.* 2018). In order to consider this proposal, *ad-hoc* hypotheses are invoked, which allude to the juxtaposition of two metamorphic events or more probably the internal dynamics of the orogenic wedge. If so, it may be possible that: (i) thrusting and very low-grade metamorphism affecting the Bahía de la Lancha Formation is younger than the low-grade metamorphism of the rest of EAMCn, or (ii) there is an out-of-sequence phase of thrusting.

Finally, it appears that both proposals for the EAMCn present difficulties in reconciling the pattern of metamorphism and structural style with middle to late Palaeozoic regional tectonic models. A conciliatory approach could thus be to combine them into a new model. In this way, the forearc position of the EAMCn for the Devonian-Carboniferous times (e.g. Suárez *et al.* 2019), as well as the findings of oceanic crust with influence of subduction (Rojo *et al.* 2020, 2021), which could be classified as supra-subduction zone ophiolites (Dilek and Furnes 2014; Furnes and Dilek 2022), lead to reconciling the previous model by considering novel tectonic models of forearc hyperextension (Fig. 10) (Maffione *et al.* 2015; van Hinsbergen *et al.* 2015; Suárez *et al.* 2022). This kind of setting, characterized by meta-pillow lavas interbedded with slates, or metamafic-ultramafic in fault contact, have also been identified in the evolution of Cenozoic forearc basins (e.g. Traiguén Basin) along the Andes (Hervé *et al.* 1995, 2017; Encinas *et al.* 2016; Suárez *et al.* 2022). Likewise, similar lithological associations have been described along the Middle-to-late Palaeozoic margin of western Gondwana from 38° S up to 44° S (e.g. Hervé *et al.* 2016; Plissart *et al.* 2019; Rapela *et al.* 2021), which is in line with the extensional kinematics of the entire margin during that time (e.g. Oriolo *et al.* 2023). Then, the metaturbidite-metabasic successions were folded and emplaced by brittle-ductile shear zones over the continent during the Gondwanide orogeny (late Palaeozoic), an orogenic event linked in southern Patagonia to the interaction with the Antarctic Peninsula terrane (Fig. 10) (e.g. Suárez *et al.* 2021, Riley *et al.* 2023).

Conclusion

Based on the quantification of very low-grade metamorphic conditions and its relationship with the structural development history identified for the Bahía de la Lancha Formation (EAMCn), we obtain two main conclusions:

- The metamorphic conditions obtained through illite crystallinity indicate values in the transition between the metapelitic zones of Lower-to-Upper Anquize, which is broadly coincident with temperatures around 250 °C.
- The structural style of deformation is akin to a fold-thrust belt. The folds and thrusts indicate a northward vergence. Taking into account the geothermal gradient proposal by previous authors, folding and thrusting might have evolved at a depth of 10 km.

Then, we recognized that previous tectonic models explaining the evolution of the EAMCn -passive margin basin incorporate into an accretionary prism or a fold-thrust belt formed during back-arc basin closure-, fail to integrate the metamorphic and structural features into the regional tectonic context. Therefore, the most parsimonious approach is to integrate both schemes into a framework of forearc hyperextension basin, which is closed during an episode of folding and thrusting, explaining all observed features. The upcoming studies will concentrate on unravelling the absolute chronology of thrusting and folding to determine whether they are related to single progressive or multiphase history of structural development.

Acknowledgment

We are grateful to Pedro from La Lila Farm for granting access to the outcrops, as well as with the Administración de Parques Nacionales Argentina for granting access and sample permit (31-DRPA). We thank the Editor Yildirim Dilek and the anonymous reviewer for the detailed review of the manuscript and the enriching comments.

Funding

Financial support was provided by the projects MINCYT-BMBFAL/17/02 and PICT-2020-SERIEA-03277 both assigned to MCG, and the PICTO-2021-YPF-CUENCA-00009 assigned to JJP.

Data availability statement

The data generated or analysed during this study are included in this published article (and its supplementary information file). Additionally, the XRD analytical results can be requested from the corresponding author.

References

1. Árkai, P., 1991. Chlorite crystallinity: an empirical approach and correlation with illite crystallinity, coal rank and mineral facies as exemplified by Palaeozoic and Mesozoic rocks of Northeast Hungary. *Journal of Metamorphic Geology* 9, 723–734.
2. Augustsson, C., Bahlburg, H., 2003. Active or passive continental margin? Geochemical and Nd isotope constraints of metasediments in the backstop of a pre-Andean accretionary wedge in southernmost Chile (46°30' – 48°30'S). In: Mc.Cann, T., Saintot, A. (Eds.), *Tracing Tectonic Deformation Using the sedimentary record*. Geological Society of London, Special Publications 253-268. doi: 10.1144/GSL.SP.2003.208.01.12.
3. Augustsson, C., Bahlburg, H., 2008. Provenance of late Palaeozoic metasediments of the Patagonian proto-Pacific margin (southernmost Chile and Argentina). *International Journal of Earth Sciences*, 97, 71-88. doi: 10.1007/s00531-006-0158-7.
4. Augustsson, C., Münker, C., Bahlburg, H., Fanning, M. 2006. Provenance of late Palaeozoic metasediments of the SW South American Gondwana margin: a combined U–Pb and Hf-isotope study of single detrital zircons. *Journal of the Geological Society*, 163, 983-995. doi: <https://doi.org/10.1144/0016-76492005-149>.
5. Allmendinger, R.W., Cardozo, N., Fisher, D., 2012, *Structural geology algorithms: Vectors and tensors in structural geology*: Cambridge University Press.

6. Ballivián Justiniano, C.A., Oriolo, S., Basei, M., 2023. Coupled U–Pb and Lu–Hf zircon data of Late Devonian magmatism from Bajo de La Leona (Deseado Massif, Argentina): Tracking the southernmost exposure of the Devonian magmatic arc of Patagonia. *Journal of South American Earth Sciences*, 128, 15, 104455. DOI: 10.1016/j.jsames.2023.104455
7. Bell, C.M., Suárez, M., 2000. The Río Lácteo Formation of southern Chile. Late Paleozoic orogeny in the Andes of southernmost South America. *J. S. Am. Earth Sci.* 13, 133–145.
8. Calderón, M., Hervé, F., Fuentes, F., Fosdick, J. C., Sepúlveda, F., Galaz, G., 2016. Tectonic Evolution of Palaeozoic and Mesozoic Andean Metamorphic Complexes and the Rocas Verdes Ophiolites in Southern Patagonia. In: Ghiglione, M.C. (Ed.), *Geodynamic Evolution of the Southernmost Andes*. Springer Earth System Sciences, 7-36. https://doi.org/10.1007/978-3-319-39727-6_2.
9. Calderón, M., Fosdick, J.C., Warren, C., Massonne, H-J., Fanning, C.M., Fadel Cury, L., Schwanethal, J., Fonseca, P.E., Galaz, G., Gaytán, D., Hervé, F., 2012. The low-grade Canal de las Montañas Shear Zone and its role on the tectonic emplacement of the Sarmiento Ophiolitic Complex and Late Cretaceous Patagonian Andes orogeny, Chile. *Tectonophysics*, 524–525, 165–185
10. Coombs, D.S., 1961. Some recent work on the lower grades of metamorphism, *Aust. J. Sci.* 24, 203-215.
11. de Barrio, R.E., Recio, C., Ríos, F.J., Rolando, A.P., Del Blanco, M.A., Schalamuk, I.B., 2023. Geology, geochemistry, isotope geochemistry and fluid inclusions of the Early Carboniferous granitic rocks from Bajo de La Leona, Deseado Massif (Santa Cruz, Argentina) and geological relationships with the Triassic-Jurassic magmatism. *J. S. Am. Earth Sci.* 123, 104197.
12. De La Cruz, R., Suárez, M., 2006. Geología del área Puerto Guadal- Puerto Sánchez, Región Aisén del General Carlos Ibáñez del Campo, Escala 1:100.000, Carta Geológica de Chile, Serie Geología Básica, No. 95. Servicio Nacional de Geología y Minería, Santiago, Chile.
13. Dylek, Y., Furnes, H., 2014. Ophiolites and their origins. *Elements*, 10, 93-100. DOI: 10.2113/gselements.10.2.93
14. Encinas, A., Folguera, A., Oliveros, V., De Girolamo Del Mauro, L., Tapia, F., Rizzo, R., Hervé, F., Finger, K.L., Valencia, V.A., Gianni, G., and Álvarez, O., 2016, Late Oligocene–early Miocene submarine volcanism and deep-marine sedimentation in an extensional basin of southern Chile: Implications for the tectonic development of the North Patagonian Andes: *Geological Society of America Bulletin*, 128, 807–823. doi:10.1130/B31303.1.

15. Falco, J.I., Hauser, N., Scivetti, N., Reimold, W.U., Schmitt, R.T., Folguera, A., 2022. Upper Triassic to Middle Jurassic magmatic evolution of northern Patagonia: Insights from the tectonic and crustal evolution of the Los Menucos area, North Patagonian Massif, Argentina. *Journal of South American Earth Sciences*, 113, 103631. [10.1016/j.jsames.2021.103631](https://doi.org/10.1016/j.jsames.2021.103631)
16. Forsythe, R., 1982. The late Palaeozoic to early Mesozoic evolution of southern South America: a plate tectonic interpretation. *Journal of the Geological Society*, 139, 671-682. <https://doi.org/10.1144/gsjgs.139.6.0671>.
17. Fossen, H., 2020. Writing papers with an emphasis on structural geology and tectonics: advices and warnings. *Brazilian Journal of Geology, Rapid communications*, 49, 4, 1-6. doi:10.1590/2317-4889201920190109
18. Fossen, H., Cavalcante, G.C.G., Pinheiro, R.B.L., Archanjo, C.J., 2019. Deformation–Progressive or multiphase?. *Structural Geology* 125, 82-99.
19. Furnes, H., Dylek, Y., 2022. Archean versus Phanerozoic oceanic crust formation and tectonics: Ophiolites through time. *Geosystems and Geoenvironment*, 1, 100004.
20. Gallardo Jara, R.E., Ghiglione, M.C., Rojas Galliani, L., Mpodozis, C., 2022. From rift to foreland basin: A case example from the Magallanes-Austral Basin, southernmost Andes. *Basin Research*, 35, 3, 865-897. <https://doi.org/10.1111/bre.12739>
21. Ghiglione, M.C., Ronda, G., Suárez, R. J., Aramendía, I., Barberón, V., Ramos, M.E., Tobal, J., García Morabito, E., Martinod, J., Sue, C., 2019. Structure and tectonic evolution of the South Patagonian fold and thrust belt: Coupling between subduction dynamics, climate and tectonic deformation. *Andean Tectonics*, 24, 675–697. <https://doi.org/10.1016/B978-0-12-816009-1.00024-1>
22. Giacosa, R.E., 1987. Micro y Mesopliegues y litología de la Formación Río Lácteo en el área de lago Belgrano, provincia de Santa Cruz. Estudio preliminar. IV Jornadas de Microtectónica. San Juan. Actas, pp. 37–41.
23. Giacosa, R.E., Fracchia, D., Heredia, N., 2012. Structure of the Southern Patagonian Andes at 49°S, Argentina. *Geologica Acta*, 10, 3, 265-282.
24. Giacosa, R.E., Márquez, M., 2002. El basamento Paleozoico de la Cordillera Patagónica. In: Haller, M.J. (Ed.), *Geología y Recursos Naturales de Santa Cruz. El Calafate* (Buenos Aires), vol. 1. Relatorio del 15° Congreso Geológico Argentino, pp. 45–55.
25. Guido, D.M., Escayola, M.P., Schalamuk, I.B., 2004. The basement of the Deseado massif at bahía Laura, Patagonia, Argentina: a proposal for its evolution. *J. S. Am. Earth Sci.* 16, 567–577.
26. Guido, D.M., Rapela, C.W., Pankhurst, R.J., Fanning, C.M., 2005. Edad del granito del afloramiento Bahía Laura, Macizo del Deseado, provincia de Santa Cruz. In: 16 Congreso Geológico Argentino, Buenos Aires, Actas, 1, pp. 85–88.

26. González, P. D., Naipauer, M., Sato, A. M., Varela, R., Basei, M. A. S., Cábana, M. C., ... Parada, M., 2020. Early Paleozoic structural and metamorphic evolution of the Transpatagonian Orogen related to Gondwana assembly. *International Journal of Earth Sciences*. doi:10.1007/s00531-020-01939-0
27. Hervé, F., Aguirre, L., Sepúlveda, V., Morata, D., 1999. Contrasting geochemistry and metamorphism of pillow basalts in metamorphic complexes from Aysén, S. Chile. *J. S. Am. Earth Sci.* 12, 379–388.
28. Hervé, F., Calderon, M., Fanning, C.M., Pankhurst, R.J., Fuentes, F., Rapela, C.W., Correa, J., Quezada, P., Marambio, C., 2016. Devonian magmatism in the accretionary complex of southern Chile. *Journal of the Geological Society*, 173, 587–602. doi:10.1144/jgs2015-163.
29. Hervé, F., Calderón, M., Faúndez, V., 2008. The metamorphic complexes of the Patagonian and Fuegian Andes. *Geologica Acta*, 6, 1, 43-53. <http://dx.doi.org/10.1344/105.000000240>.
30. Hervé, F., Fanning, C.M., Pankhurst, R.J., 2003. Detrital zircon age patterns and provenance of the metamorphic complexes of southern Chile. *Journal of South American Earth Sciences*, 16, 107–123. [https://doi.org/10.1016/S0895-9811\(03\)00022-1](https://doi.org/10.1016/S0895-9811(03)00022-1).
31. Hervé, F., Fuentes, F., Calderón, M., Fanning, C.M., Quezada, P., Pankhurst, R.J., Rapela, C.W., 2017. Ultramafic rocks in the North Patagonian Andes: is their emplacement associated with the Neogene tectonics of the Liquiñe-Ofqui Fault Zone? *Andean Geology*, 44, 1, 1-16. Doi: 10.5027/andgeoV44n1-a01.
32. Hervé, F., Pankhurst, R.J., Drake, R., Beck, M.E., 1995, Pillow metabasalts in a mid-tertiary extensional basin adjacent to the Liquiñe-Ofqui fault zone: The Isla Magdalena area, Aysén, Chile. *Journal of South American Earth Sciences*, 8, 33–46. doi:10.1016/0895-9811(94)00039-5.
33. Hueck, M., Wemmer, K., Ksienzyk, A.K., Kuehn, R., Vogel, N., 2022. Potential, premises, and pitfalls of interpreting illite argon dates - A case study from the German Variscides. *Earth-Science Reviews*, 232, 104133. <https://doi.org/10.1016/j.earscirev.2022.104133>
34. Hueck, M., Wemmer, K., Basei, M.A., ... & Siegesmund, S. (2020). Dating recurrent shear zone activity and the transition from ductile to brittle deformation: White mica geochronology applied to the Neoproterozoic Dom Feliciano Belt in South Brazil. *Journal of Structural Geology*, 141, 104199.
35. Klepeis, K., Betka, P., Clarke, G., Fanning, C.M., Hervé, F., Rojas, L., Mpodozis, C., Thomson, S.N., 2010. Continental underthrusting and obduction during the Cretaceous closure of the Rocas Verdes rift basin, Cordillera Darwin, Patagonian Andes. *Tectonics*, 29, TC3014.

36. Kübler, B., 1968. Evaluation quantitative du métamorphisme par la cristallinité d'illite. *Bull. Centre Rech. Pau - S.N.P.A.* 2, 385-397.
37. Kübler, B., Jaboyedoff, M., 2000. Illite crystallinity. *Comptes Rendus de l'Academie de Sciences- Serie IIa: Sciences de la Terre et des Planetes* 331, 75–89.
38. Lacassie, J.P., 2003. Estudio de la Proveniencia Sedimentaria de los Complejos Metamórficos de los Andes Patagónicos (46°-51° Lat. S), mediante la aplicación de redes neuronales e isótopos estables. Doctoral Thesis. Universidad de Chile, 119 pp.
39. Lanari, P., Engi, M., 2017. Local bulk composition effects on metamorphic mineral assemblages. *Reviews in Mineralogy and Geochemistry* 83, 55–102.
40. Maffione, M., van Hinsbergen, D.J.J., Koornneef, L.M.T., Guilmette, C., Hodges, K., Borneman, N., Huang, W., Ding, L., Kapp, P., 2015. Forearc hyperextension dismembered the south Tibetan ophiolites. *Geology*, 43, 6, 475–478. <https://doi.org/10.1130/G36472.1>.
41. Malkowsky, M.A., Groove, M., Graham, S.A., 2016. Unzipping the Patagonian Andes—Long-lived influence of rifting history on foreland basin evolution. *Lithosphere, Short Research*, 8, 1, 23–28.
42. Merriman, R.J., Frey, M., 1999. Patterns of Very Low-Grade Metamorphism in Metapelitic Rocks. In: *Low-Grade Metamorphism* (Frey, M., and Robinson, D., eds). Blackwell Publishing Ltd., 313p.
43. Merriman, R.J., Roberts, B., 1995. Low-grade metamorphism of the Lower Palaeozoic sequence. In: *The Geology of the Rhins of Galloway District* (ed. P. Stone), pp. 6770. Memoir of the British Geological Survey, sheets 1 and 3 (Scotland).
44. Millar, I.L., Pankhurst, R.J., Fanning, C.M., 2002. Basement chronology of the Antarctic Peninsula: recurrent magmatism and anatexis in the Palaeozoic Gondwana margin. *Geol Soc London* 159, 145–157.
45. Moore, D.M., Reynolds, R.C., 1997. *X-Ray Diffraction and the Identification and Analysis of Clay Minerals*. Oxford University Press, 378 pp.
46. Moreira, P., Fernández, R., Hervé, F., Fanning, C.M., Schalamuk, I.A., 2013. Detrital zircons U–Pb SHRIMP ages and provenance of La Modesta Formation, Patagonia Argentina. *J. S. Am. Earth Sci.* 47, 32–46.
47. Muller, V., Calderón, M., Fosdick, J.C., Ghiglione, M.C., Cury, L.F., Massonne, H.-J., Fanning, C.M., Warren, C.J., Ramírez de Arellano, C., Sternai, P., 2021. The closure of the Rocas Verdes Basin and early tectono-metamorphic evolution of the Magallanes fold-and-thrust belt, southern Patagonian Andes (52–54°S). *Tectonophysics*, 798. <https://doi.org/10.1016/j.tecto.2020.228686>.
48. Oriolo, S., Schulz, B., Hueck, M., ... & Siegesmund, S. 2022. The petrologic and petrochronologic record of progressive vs polyphase deformation: Opening the analytical

toolbox. Earth-Science Reviews, 234, 104235.
<https://doi.org/10.1016/j.earscirev.2022.104235>

49. Oriolo, S., González, P.D., Renda, E.M., Basei, M.A.S., Otamendi, J., Cordenons, P., Marcos, P., Yoya, M.B., Ballivián Justiniano, C.A., Suárez, R., 2023. Linking accretionary orogens with continental crustal growth and stabilization: Lessons from Patagonia. *Gondwana Research*, 121, 368–382.
50. Pankhurst, R.J., Rapela, C.W., Loske, W.P., Marquez, M., Fanning, C.M., 2003. Chronological study of the pre-Permian basement rocks of southern Patagonia. *Journal of South American Earth Sciences*, 16, 27–44.
51. Poiré, D.G., Morel, E., Maggi, J.H., 1999. Facies diamictíticas en la Formación Bahía de la Lancha (Paleozoico), Estancia La Lila, Lago San Martín, provincia de Santa Cruz, Argentina. In: XIV Congreso Geológico Argentino, Salta, Actas 1: 425–428.
52. Permuy Vidal, C., Moreira, P., Guido, D.M., Fanning, C.M., 2014. Linkages between the southern Patagonia pre-Permian basements: new insights from detrital zircons U-Pb SHRIMP ages from the Cerro Negro District. *Geol. Acta*, 12, 2, 137–150.
53. Plissart, G., González-Jiménez, J.M., Garrido, L.N., Colás, V., Berger, J., Monnier, C., Diot, H., Padrón-Navarta, J.A., 2019. Tectono-metamorphic evolution of subduction channel serpentinites from South-Central Chile. *Lithos* 336, 221–241.
54. Ramírez-Sánchez, E., Hervé, F., Kelm, U., Sassi, R., 2005. P-T conditions of metapelites from metamorphic complexes in Aysen, Chile. *Journal of South American Earth Sciences*, 19, 373–386.
55. Ramos, V. A., 1982. Descripción geológico-económica de las Hojas 53 a, Cerro San Lorenzo y 53 b, Meseta Belgrano, provincia de Santa Cruz. Servicio Geológico Nacional (unpublished).
56. Ramos, V.A., 2008. Patagonia: a Paleozoic continent adrift? *J. S. Am. Earth Sci.* 26, 235–251. <https://doi.org/10.1016/j.jsames.2008.06.002>
57. Rapela, C.W., Hervé, F., Pankhurst, R.J., Calderón, M., Fanning, C.M., Quezada, P., Poblete, F., Palape, C., Reyes, T., 2021. The Devonian accretionary orogen of the North Patagonian cordillera. *Gondwana Research*, 96, 1–21.
58. Renda, E., Alvarez, D., Prezzi, C., Oriolo, S., Vizán, H., 2019. Inherited basement structures and their influence in foreland evolution: A case study in Central Patagonia, Argentina. *Tectonophysics*, 772, 228232.
59. Renda, E., González, P.D., Vizán, H., Oriolo, S., Prezzi, C., González, V.R., Schulz, B., Krause, J., Basei, M., 2021. Igneous-metamorphic basement of Taquetrén Range, Patagonia, Argentina: A key locality for the reconstruction of the Paleozoic evolution of Patagonia. *Journal of South American Earth Sciences*, 106, 103045.

60. Riccardi, A., 1971. Estratigrafía en el oriente de la Bahía de la Lancha, Lago San Martín, Santa Cruz, Argentina. *Revista Museo de la Plata*, 61, 7, 245–318.
61. Riley, T.R., Burton-Johnson, A., Flowerdew, M.J., Poblete, F., Castillo, P., Hervé, F., Leat, P., Millar, I.L., Bastias, J., Whitehouse, M.J., 2023. Palaeozoic – Early Mesozoic geological history of the Antarctic Peninsula and correlations with Patagonia: Kinematic reconstructions of the proto-Pacific margin of Gondwana. *Earth-Science Reviews*, 236, 2023, 104265. <https://doi.org/10.1016/j.earscirev.2022.104265>
62. Riley, T.R., Flowerdew, M.J., Whitehouse, M.J., 2012. U–Pb ion-microprobe zircon geochronology from the basement inliers of eastern Graham Land, Antarctic Peninsula. *Journal of the Geological Society*, 169, 381 –393. doi: 10.1144/0016-76492011-142.
63. Robinson, D., Bevins, R.E., 1989. Diastathermal (extensional) metamorphism at very low grades and possible high grade analogues. *Earth and Planetary Science letters*, 92, 81-88.
64. Robinson, D., Bevins, R.E., 1999. Patterns of Regional Low-Grade Metamorphism in Metabasites. In: *Low-Grade Metamorphism* (Frey, M., and Robinson, D., eds). Blackwell Publishing Ltd., 313p.
65. Robinson, D., Merriman, R.J., 1999. Low-Temperature Metamorphism: An Overview. In: *Low-Grade Metamorphism* (Frey, M., and Robinson, D., eds). Blackwell Publishing Ltd., 313p.
66. Rojo, D., Díaz, J., Quezada, P., Suárez, R.J., Calderón, M., Hervé, F., Fuentes, F., Ghiglione, M., Theye, T., Viefhaus, T., Cataldo, J., 2020. Tectonic significance of Palaeozoic metabasic and serpentinites rocks of Igneous and Metamorphic Complex Leon in the northern Eastern Andean Metamorphic Complex (46-47°S), Chile. *Journal of South American Earth Sciences*, 108, 103198.
67. Rojo, D., Calderón, M., Ghiglione, M. C., Suárez, R. J., Quezada, P., Cataldo, J., ... Babinski, M., 2021. The low-grade basement at Península La Carmela, Chilean Patagonia: new data for unraveling the pre-Permian basin nature of the Eastern Andean Metamorphic Complex. *International Journal of Earth Sciences*, 110, 6, 2021–2042. doi:10.1007/s00531-021-02054-4
68. Sample, J.C., Moore, J.C., 1987. Structural style and kinematics of an underplated slate belt, Kodiak and adjacent islands, Alaska. *Geological Society of America Bulletin*, 99, 7-20.
69. Serra-Varela, S., Heredia, N., Giacosa, R., García-Sanseguundo, J., Farias, P., 2020. Review of the polyorogenic Palaeozoic basement of the Argentinean North Patagonian Andes: age, correlations, tectonostratigraphic interpretation and geodynamic evolution. *International Geology Review*. <https://doi.org/10.1080/00206814.2020.1839798>

70. Seton, M., Müller, R.D., Zahirovic, S., Gaina, C., Torsvik, T., Shephard, G., Talsma, A., Gurnis, M., Turner, M., Maus, S., Chandler, M., 2012. Global continental and ocean basin reconstructions since 200 Ma. *Earth-Science Reviews*, 113, 212–270. doi:10.1016/j.earscirev.2012.03.002.
71. Shell, C.A.P.S.A., 1965. La palinología en la Industria Petrolera y algunos resultados palinológicos en la Argentina. *Segundas Jornadas Geológicas Argentinas*, 3, 347–353.
72. Suárez, R.J., Ghiglione, M.C., Sue, C., Quezada, P., Rojo, D., Calderón, M., 2021. Palaeozoic-early Mesozoic structural evolution of the West Gondwana accretionary margin in southern Patagonia, Argentina. *Journal of South American Earth Sciences*, 106, 103062. <http://dx.doi.org/10.1016/j.jsames.2020.103062>
73. Suárez, R.J., González, P.D., Ghiglione, M.C., 2019. A review on the tectonic evolution of the Palaeozoic-Triassic basins from Patagonia: Record of protracted westward migration of the pre-Jurassic subduction zone. *J. S. Am. Earth Sci.* 95, 102256.
74. Suárez, R.J., Guillaume, B., Martinod, J., Ghiglione, M.C., Sue, C., Kermarrec, J.-J., 2022. Role of convergence obliquity and inheritance on sliver tectonics: Insights from 3-D subduction experiments. *Tectonophysics*, 842, 229583. DOI: 10.1016/j.tecto.2022.229583
75. Süssenberger, A., Schmidt, S.T., Wemmer, K., Baumgartner, L.P., Grobety, B., 2018. Timing and thermal evolution of fold-and-thrust belt formation in the Ultima Esperanza District, 51°S Chile: Constraints from K-Ar dating and illite characterization. *GSA Bulletin*, 130, 5–6, 975–998. <https://doi.org/10.1130/B31766>
76. Thomson, S.N., Hervé, F., 2002. New time constraints for the age of metamorphism at the ancestral Pacific Gondwana margin of southern Chile (42–52°S). *Rev. Geol. Chile* 28 (2), 255–271.
77. Torres-Carbonel, P.J., Cao, S.J., González-Guillot, M., Mosqueira González, V., Dimieri, L.V., Duval, F., Scaillet, S., 2020. The Fuegian thrust-fold belt: From arc-continent collision to thrust-related deformation in the southernmost Andes. *Journal of South American Earth Sciences*, 102, 10267.
78. Van Hinsbergen, D.J.J., Peters, K., Maffione, M., Spakman, W., Guilmette, C., Thieulot, C., ... Kaymakci, N., 2015. Dynamics of intraoceanic subduction initiation: 2. Suprasubduction zone ophiolite formation and metamorphic sole exhumation in context of absolute plate motions. *Geochemistry, Geophysics, Geosystems*, 16, 6, 1771–1785. doi:10.1002/2015gc005745
79. Valín, M. L., García-López, S., Brime, C., Bastida, F., Aller, J., 2016. Tectonothermal evolution in the core of an arcuate fold and thrust belt: the south-eastern sector of the Cantabrian Zone (Variscan belt, north-western Spain). *Solid Earth*, 7, 1003–1022. <https://doi.org/10.5194/se-7-1003-2016>

80. Verdecchia, S.O., Collo, G., Zandomeni, P.S., Wunderlin, C., Fehrmann, M., 2021. Crystallochemical indexes and geothermobarometric calculations as a multiproxy approach to P-T condition of the low-grade metamorphism: The case of the San Luis Formation, Eastern Sierras Pampeanas of Argentina. *Lithos*, 324-325, 385-341. <https://doi.org/10.1016/j.lithos.2018.11.021>
81. Von Gosen, W., Buggisch, W., Krumm, S., 1991. Metamorphism and deformation mechanisms in the Sierras Australes fold and thrust belt (Buenos Aires Province, Argentina). *Tectonophysics*, 185, 335-356.
82. Warr, L.N., 2018. A new collection of clay mineral "Crystallinity" Index Standards and revised guidelines for the calibration of Kübler and Árkai indices. *Clay Minerals*, 53, 3, 339-350. <https://doi.org/10.1180/clm.2018.42>
83. Warr, L.N., Ferreiro Mählmann, R., 2015. Recommendations for Kübler Index standardization. *Clay Minerals*, 50, 283-286.
84. Warr, L.N., Greiling, R.O., Zachrisson, E., 1996. Thrust-related very low grade metamorphism in the marginal part of an orogenic wedge, Scandinavian Caledonides. *Tectonics*, 15, 6, 1213-1229.
85. Warr L.N., Rice A.H.N., 1994. Interlaboratory standardization and calibration of clay mineral crystallinity and crystallite size data. *Journal of Metamorphic Geology*, 12, 141-152.
86. Willner, A.P., Hervé, F., Thomson, S.N., Massonne, H-J., 2004. Converging PT-paths of Mesozoic HP-LT metamorphic units (Diego de Almagro Island, Southern Chile, 51°30'S): evidence for juxtaposition during late shortening of an active continental margin. *Miner Petrol*, 81, 43-84.
87. Yoshida, K., 1981. Estudio geológico del curso superior del río Baker, Aysén, Chile. Ph.D. thesis, Universidad de Chile, 47°05' a 47°42S' 72°28' a 73°15'W).

Table captions

Metapelitic samples			
<i>ID</i>	<i>Lat</i>	<i>Long</i>	<i>Structural domain</i>
<i>PO-01</i>	49°15'45.7"	72°56'22.9"	Footwall of the Polo thrust
<i>PO-02</i>	49°15'49.7"	72°56'23.2"	
<i>PO-03</i>	49°15'42.4"	72°56'27.1"	
<i>PO-04</i>	49°14'37.8"	72°56'32.8"	Hanging wall of the Polo thrust
<i>PO-05</i>	49°14'22.7"	72°56'20.4"	
<i>BL-05</i>	48°59'48.1"	72°13'14.7"	Hanging wall of the La Lila reverse duplex
<i>BL-07</i>	49° 0'45.27"	72°14'3.43"	
<i>BL-08</i>	48°59'58.18"	72°13'21.56"	
<i>BL-04</i>	48°59'44.6"	72°13'15"	Shear zone (cataclastic rock)
<i>BL-01</i>	48°57'05.6"	72°13'46.9"	Footwall of the La Lila reverse duplex
<i>BL-02</i>	48°57'15"	72°14'4.4"	
<i>BL-03</i>	48°58'49"	72°13'34"	
<i>BL-06</i>	48°59'37.1"	72°13'06.2"	
<i>CR-01</i>	48°54'4.10"	72°22'53.80"	Regional sampling
<i>CR-02</i>	48°54'46.00"	72°22'28.20"	

Table 1. XRD sample locations of metapelitic rocks along the Bahía de la Lancha Formation.

Sample ID	KI_{CIS} (001)	Metapelitic zone	Tectonic fabric	Structural domain
<i>PO-01</i>	0.45	Lower Anchizone	Slaty cleavage	Hanging wall of the Polo thrust
<i>PO-02</i>	0.45	Lower Anchizone	Slaty cleavage	
<i>PO-03</i>	0.39	Upper anchizone	Slaty cleavage	
<i>PO-04</i>	0.40	Upper anchizone	Pencil-like cleavage	Footwall of the Polo thrust
<i>PO-05</i>	0.42	Upper-Lower Anchizone	Pencil-like cleavage	
<i>BL-05</i>	0.42	Upper-Lower Anchizone	Pencil-like cleavage	Hanging wall of the La Lila reverse duplex
<i>BL-07</i>	0.39	Upper anchizone	Pencil-like cleavage	
<i>BL-08</i>	0.56	Upper Diagenetic zone	Cleaved	
<i>BL-04</i>	0.60	Upper Diagenetic zone	S/C foliation	Cataclastic rock of shear zone
<i>BL-01</i>	0.37	Upper anchizone	Pencil-like cleavage	Footwall of the La Lila reverse duplex
<i>BL-02</i>	0.40	Upper anchizone	Pencil-like cleavage	
<i>BL-03</i>	0.50	Lower Anchizone	Cleaved	
<i>BL-06</i>	0.51	Lower Anchizone	Pencil-like cleavage	
<i>CR-01</i>	0.34	Upper anchizone	Disharmonic folding	Regional sampling
<i>CR-02</i>	0.36	Upper anchizone	Disharmonic folding	

Table 2. K_{ICIS} values and their correlation with the metapelite zones, and further features of mesoscale tectonic fabric for the samples belonging to the Bahía de la Lancha Formation.

Figure captions

Fig. 1. Palaeogeographic reconstruction of Patagonia-Antarctic Peninsula in Pangea (at 200 Ma) (coastlines from Seton *et al.* 2012, and the position of the Antarctic Peninsula is based on Riley *et al.* 2023). Note that the EAMC occupies a forearc position with respect to the Devonian-Carboniferous Western magmatic belt (red dotted line). Consult the pre-Jurassic magmatic ages on Millar *et al.* (2002), Pankhurst *et al.* (2003), Calderón *et al.* (2010), Riley *et al.* (2012), González *et al.* (2020), Serra-Varela *et al.* (2020), Renda *et al.* (2021), Falco *et al.* (2022), Ballivián Justiniano *et al.* (2023), Oriolo *et al.* (2023), and references therein. The red ellipse outlines the location of the Eastern Andean Metamorphic Complex.

Fig. 2. Regional map of the South Patagonian Andes (based on Ramos 1972, Marquez and Giacosa 2002; Suárez *et al.* 2021). The red polygons correspond to the survey sectors by Ramírez-Sánchez *et al.* (2005) and this study, and the coloured dots depict the U-Pb maximum depositional ages obtained by Hervé *et al.* (2003), Augustsson *et al.* (2006), Malkowsky *et al.* (2016), Suárez *et al.* (2019a), and Rojo *et al.* (2021). The profile X-X' corresponds to the regional structural cross-section of Figure 3.

Fig. 3. Regional structural cross-section modified from Suárez *et al.* (2021), which was employed as the structural framework for strategical sampling of metapelitic rocks for the XRD analysis presented in this contribution. See location of profile X-X' in Figure 2.

Fig. 4. (a) and (b) Geological-structural map in detail of the stratotype locality “*La Lancha Bay*” of the Bahía de la Lancha Formation (modified from Suárez *et al.* 2021). See profile A-A’ in Figure 5. (c) The equal-area, lower-hemisphere stereograms, present data on tectonic fabric from this contribution and Suárez *et al.* (2021). The stereograms were performed with the Stereonet (v.11.) software (Allmendinger *et al.* 2012).

Fig. 5. Structural cross-section in detail to display the geometry of the La Lila duplex system. See the location of profile in Figure 4.

Fig. 6. (a) Large-scale, upright fold, involved in the frontal sector of the La Lila Duplex system. (b) Detail to exhibit the vergence towards the north of chevron folds develop in slates. The inset displays pencil-like fragments in the zone of chevron folds. (c) Cataclastic rock of shear zone exhibiting S-C fabric, which indicated top-to-N (to NE) vergence. This rock corresponds to sample BL-04.

Fig. 7. Field photography exhibiting the relationship between folds and cleavage. (a) Disharmonic folds in a succession of metapelite and metasedimentary rock of the Cancha Rayada Peninsula. (b) Axial plane slaty cleavage related with tight folds. (c) Pencil cleavage formed by the intersection between S_0 - S_{sc} planes in the hinge zone of tight folds. (d) X-Ray Diffractograms showing the illite and chlorite peaks in the BL-01 and BL-05 samples. The profiles correspond to air dry (red profile), ethylene glycol (blue profile), and heated (black profile) preparations of oriented mounts.

Fig. 8. Regional map of the South Patagonian Andes with location of sites with metamorphic constraints. In the inset, we plot P-T estimations of the EAMCn (Hervé *et al.* 1999, Ramírez-Sánchez *et al.* 2005), and also include as reference a fossil accretionary prism (Willner *et al.* 2004) and back-arc basin closure (Muller *et al.* 2020) both from southern Patagonia.

Fig. 9. Variations in the metamorphic conditions of the EAMCn in order to exhibit the trends of metamorphism. (a) Graphic of “Latitude vs. Kübler index (KI_{CIS}). (b) Graphic of “Kübler index (KI_{CIS}) vs. present-day horizontal distance to palaeo-arc magmatism”. See location of the palaeo-magmatic arc in Figure 1. It should be noted that the graphics do not include samples of Ramírez-Sánchez *et al.* (2005) located near younger plutons, in order to avoid the overprinting of thermal effects.

Fig. 10. Tectonic model explaining the middle-to-late Palaeozoic evolution of the EAMCn in the framework of (a) hyperextended forearc basin and (b) further closure linked with plate interaction of southern Patagonia-Antarctic Peninsula.

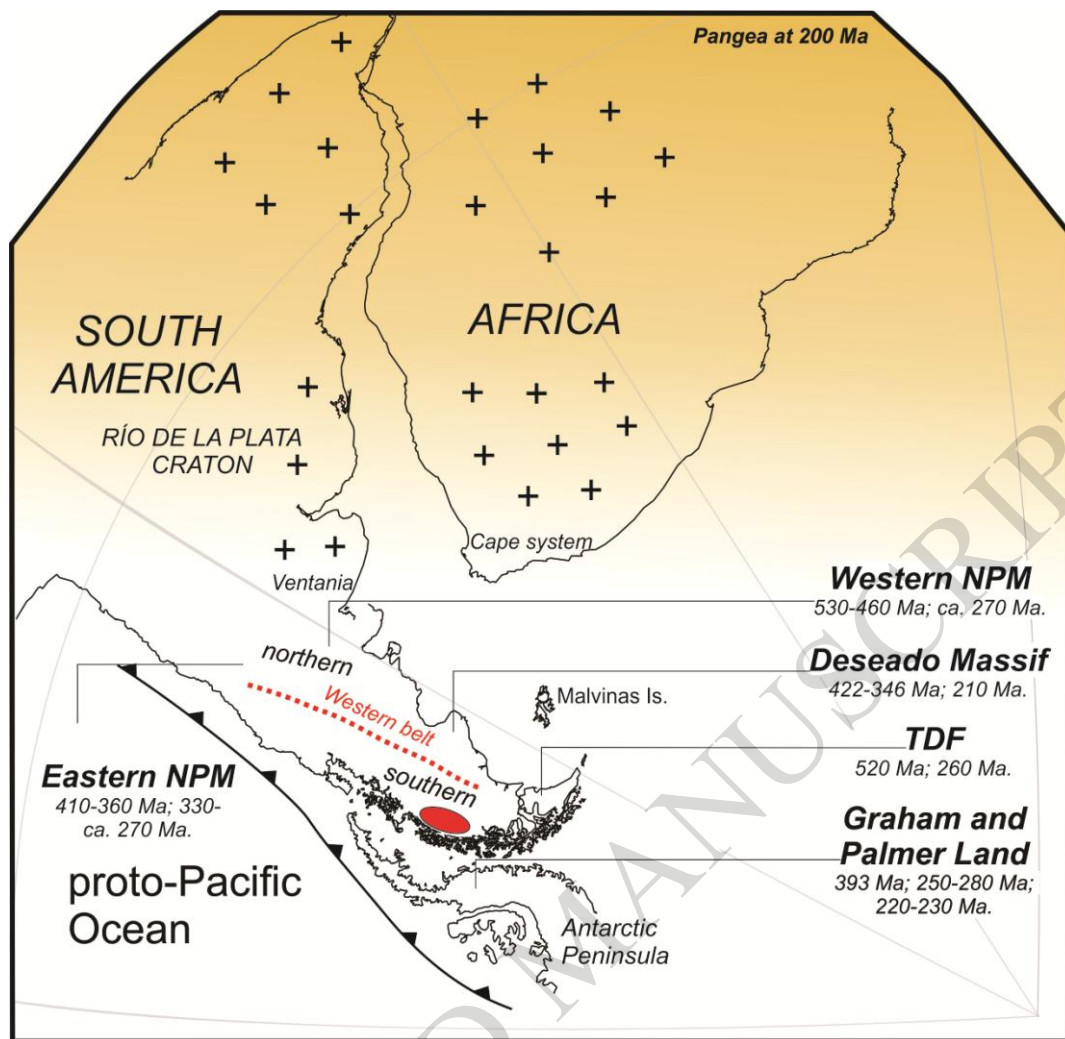


FIGURE 1

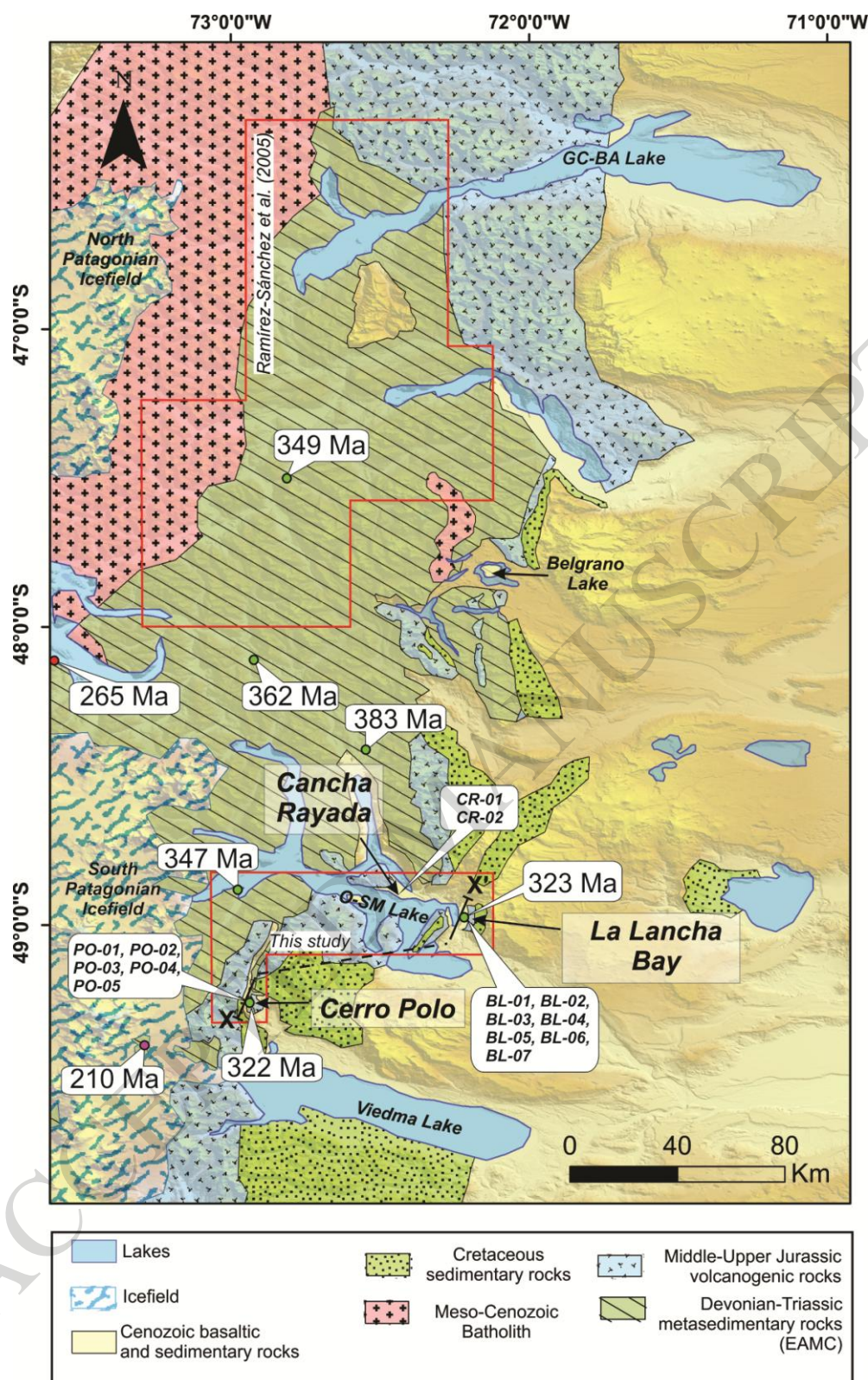


FIGURE 2

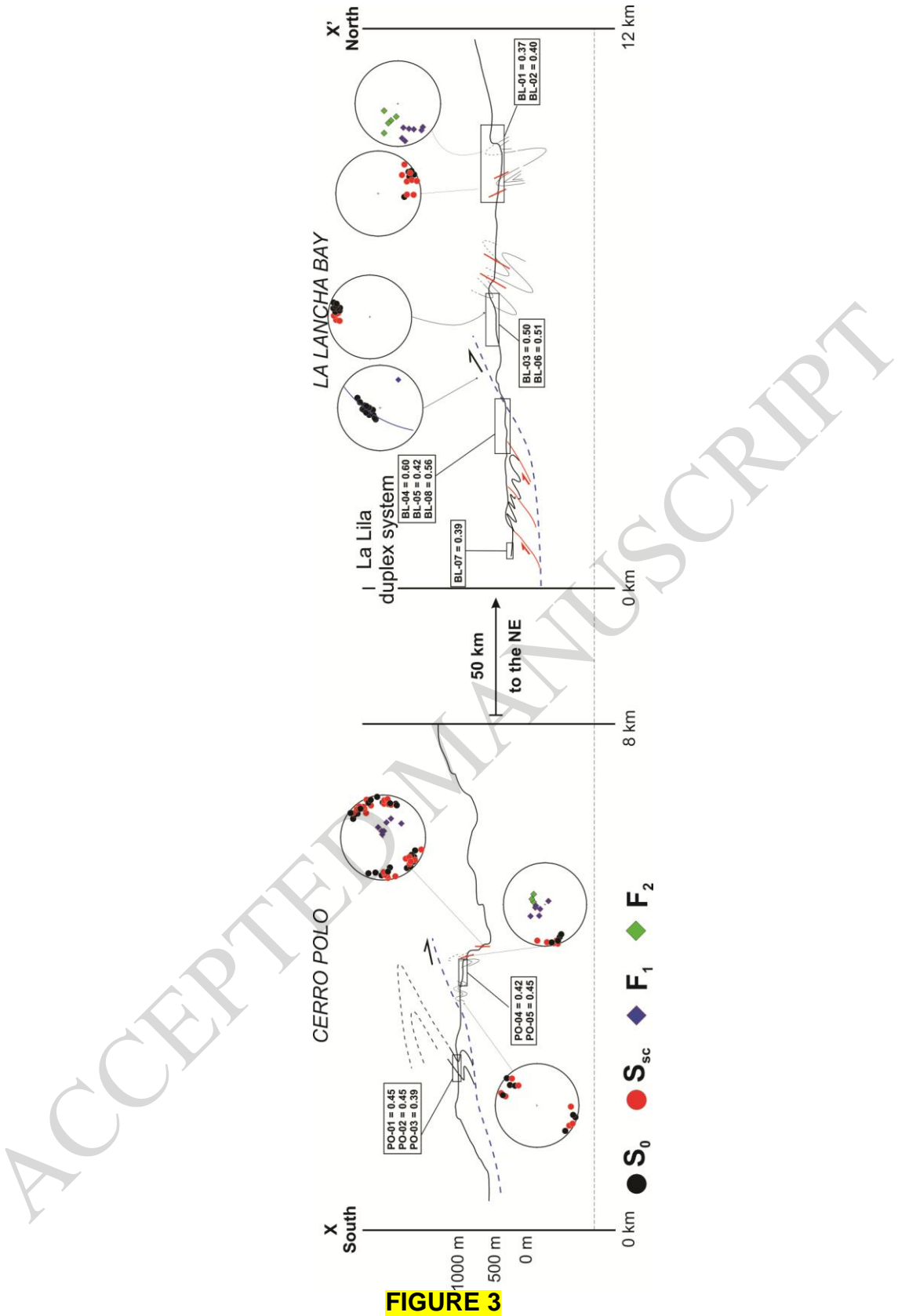
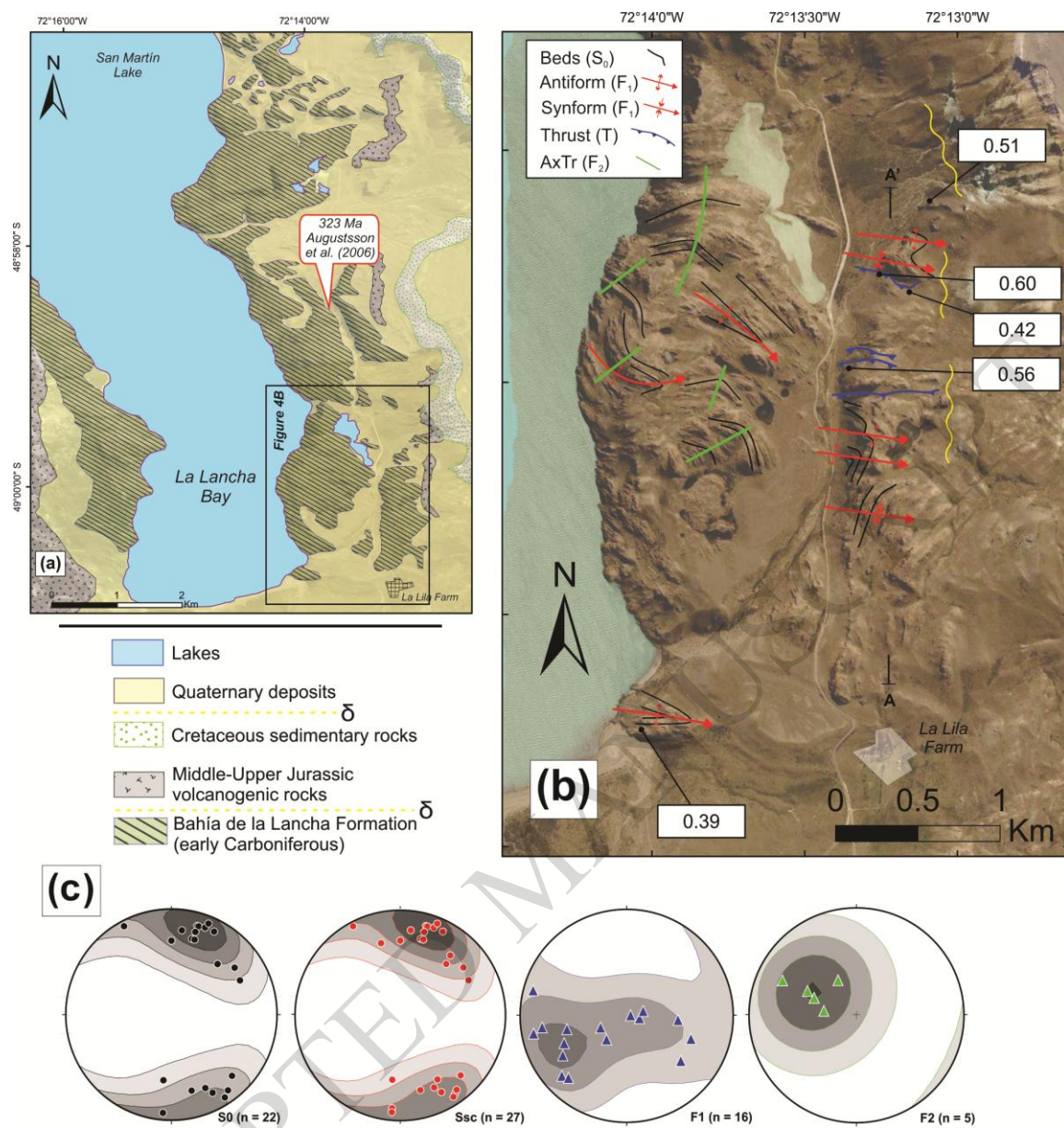


FIGURE 3

**FIGURE 4**

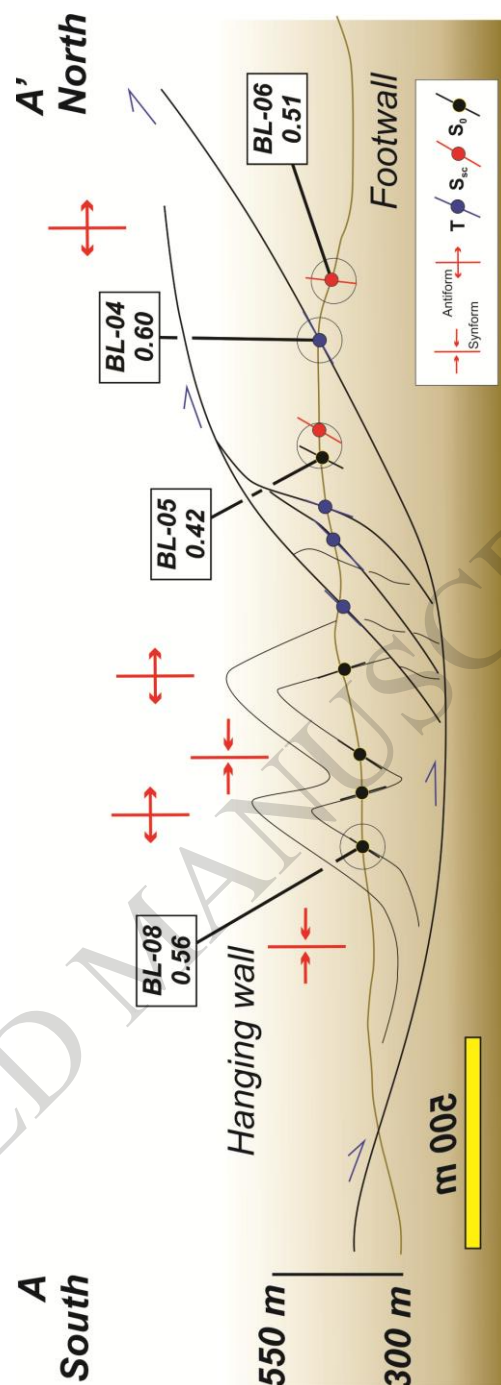


FIGURE 5

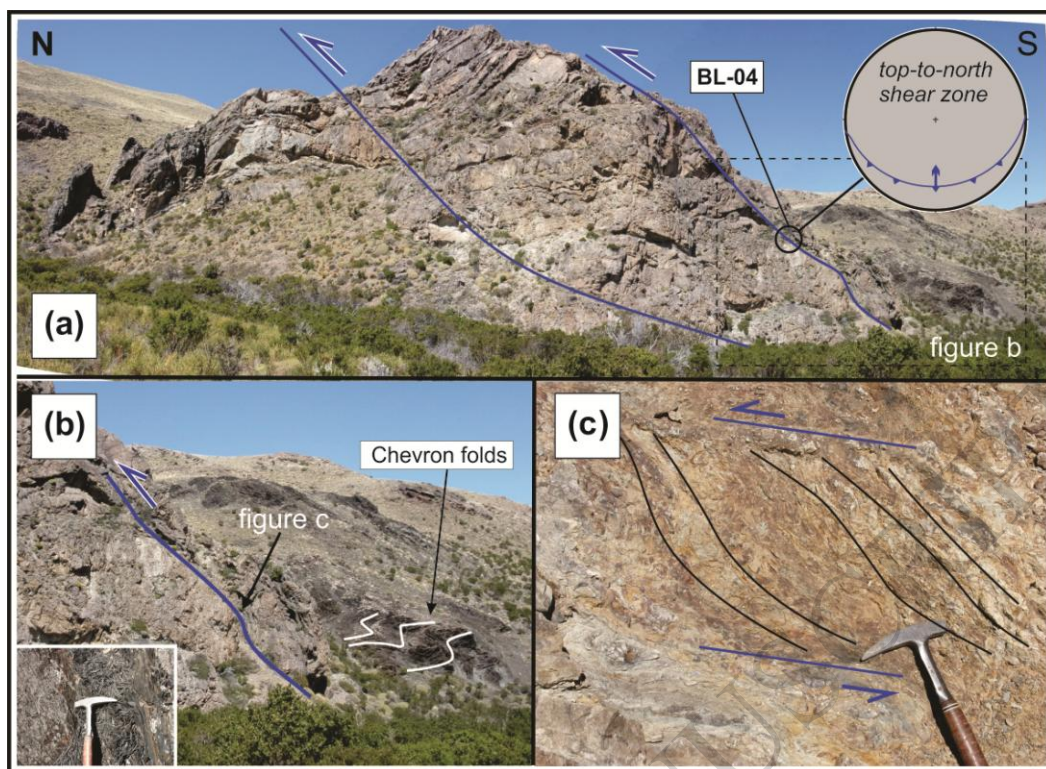


FIGURE 6

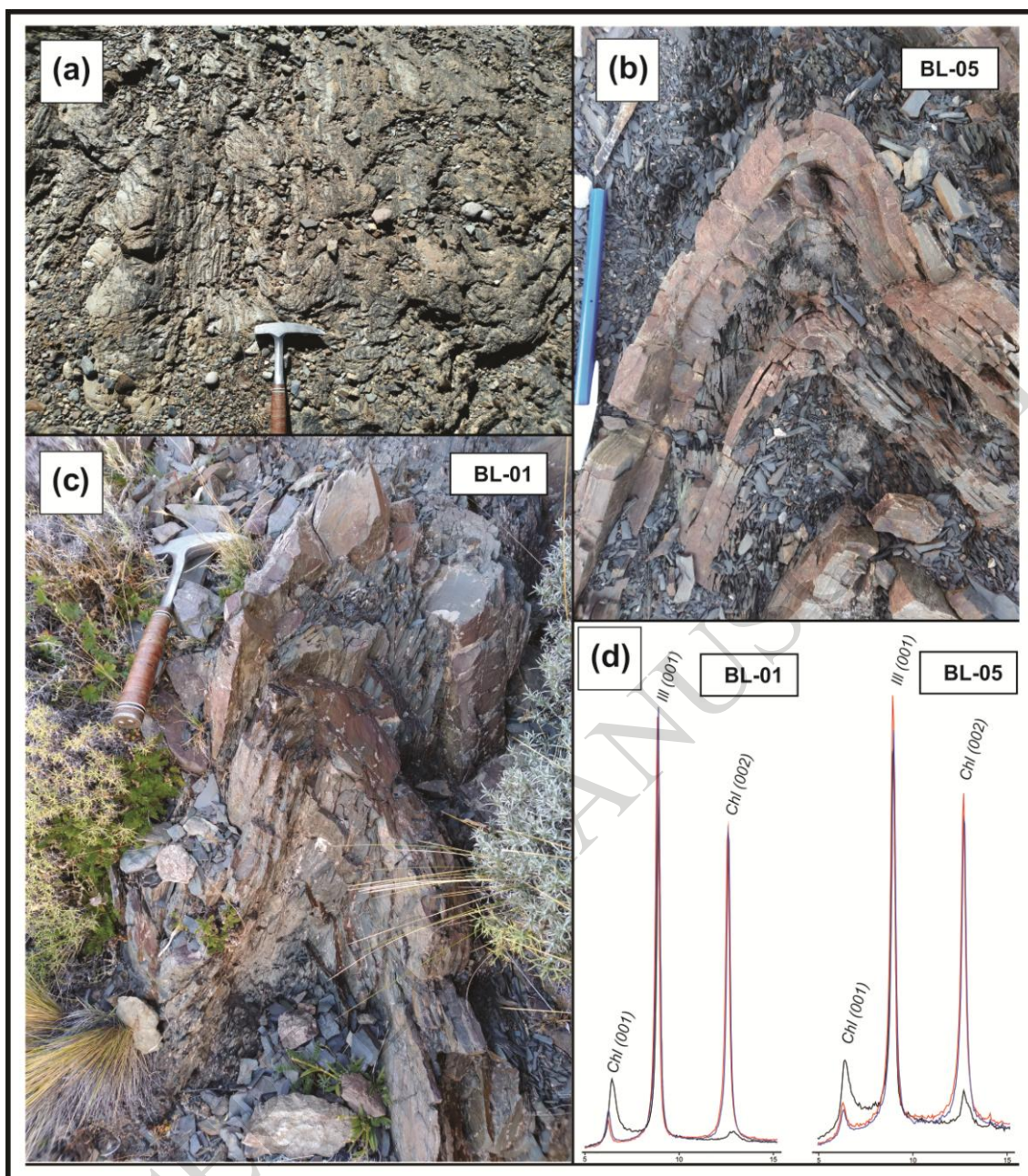


FIGURE 7

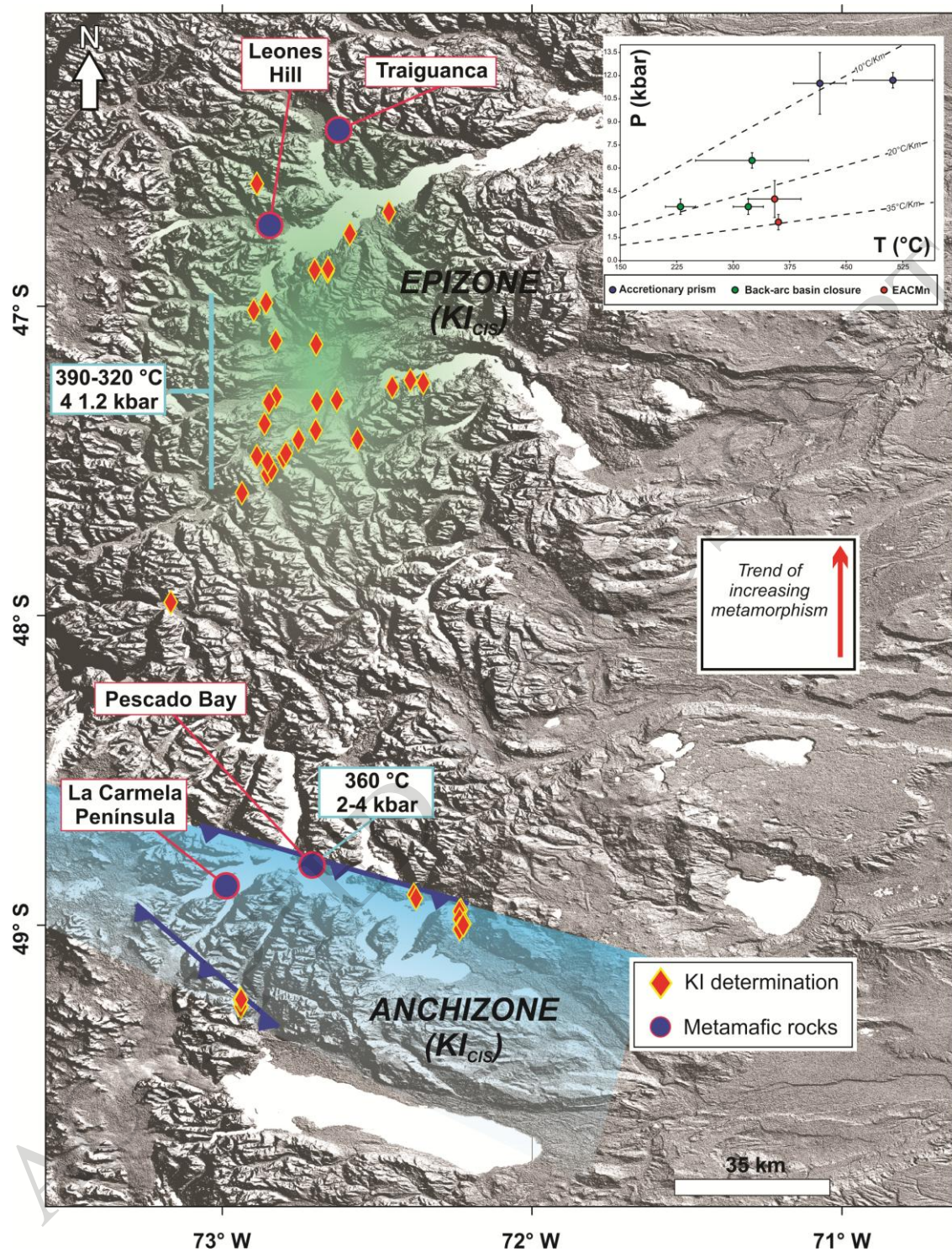


FIGURE 8

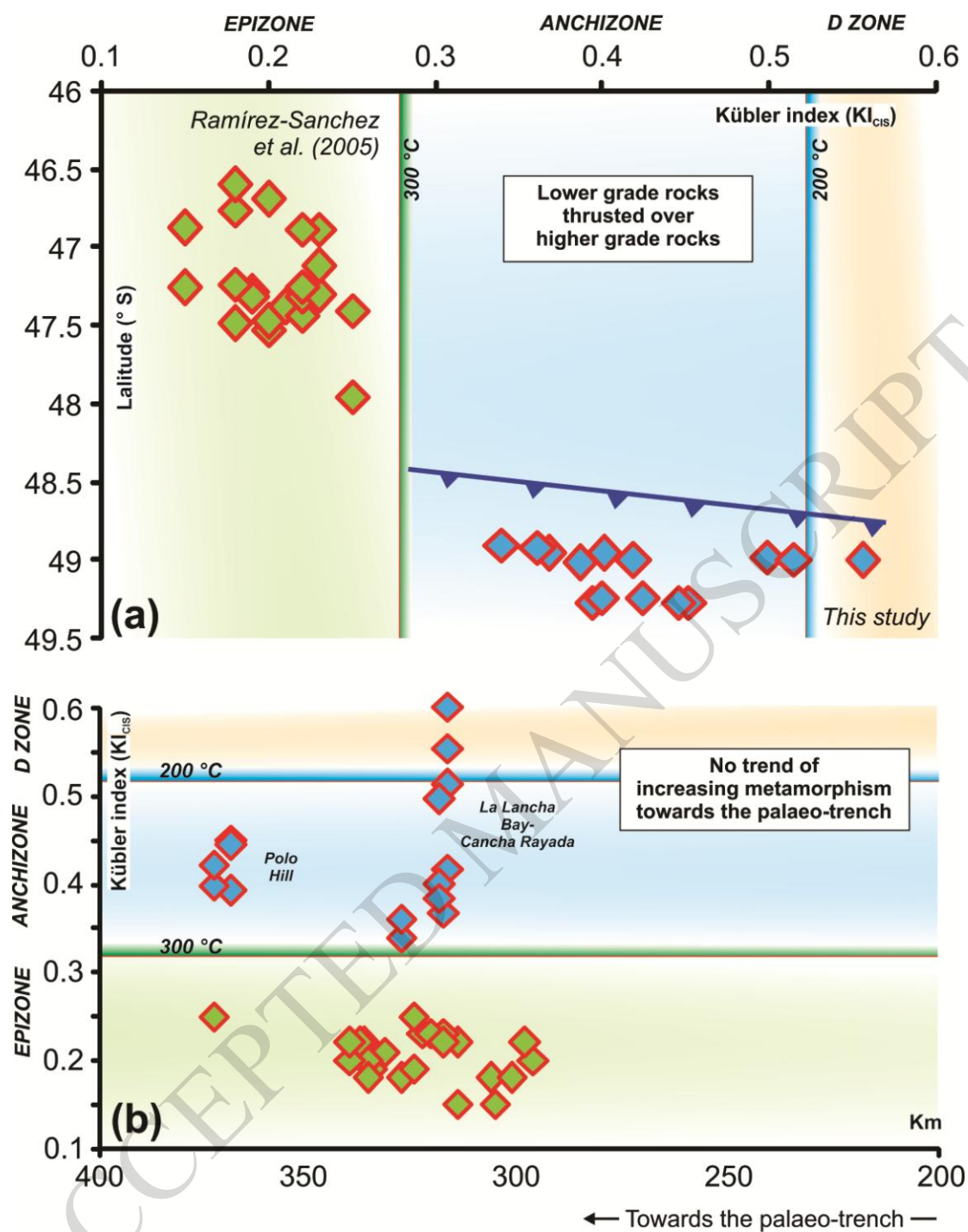


FIGURE 9

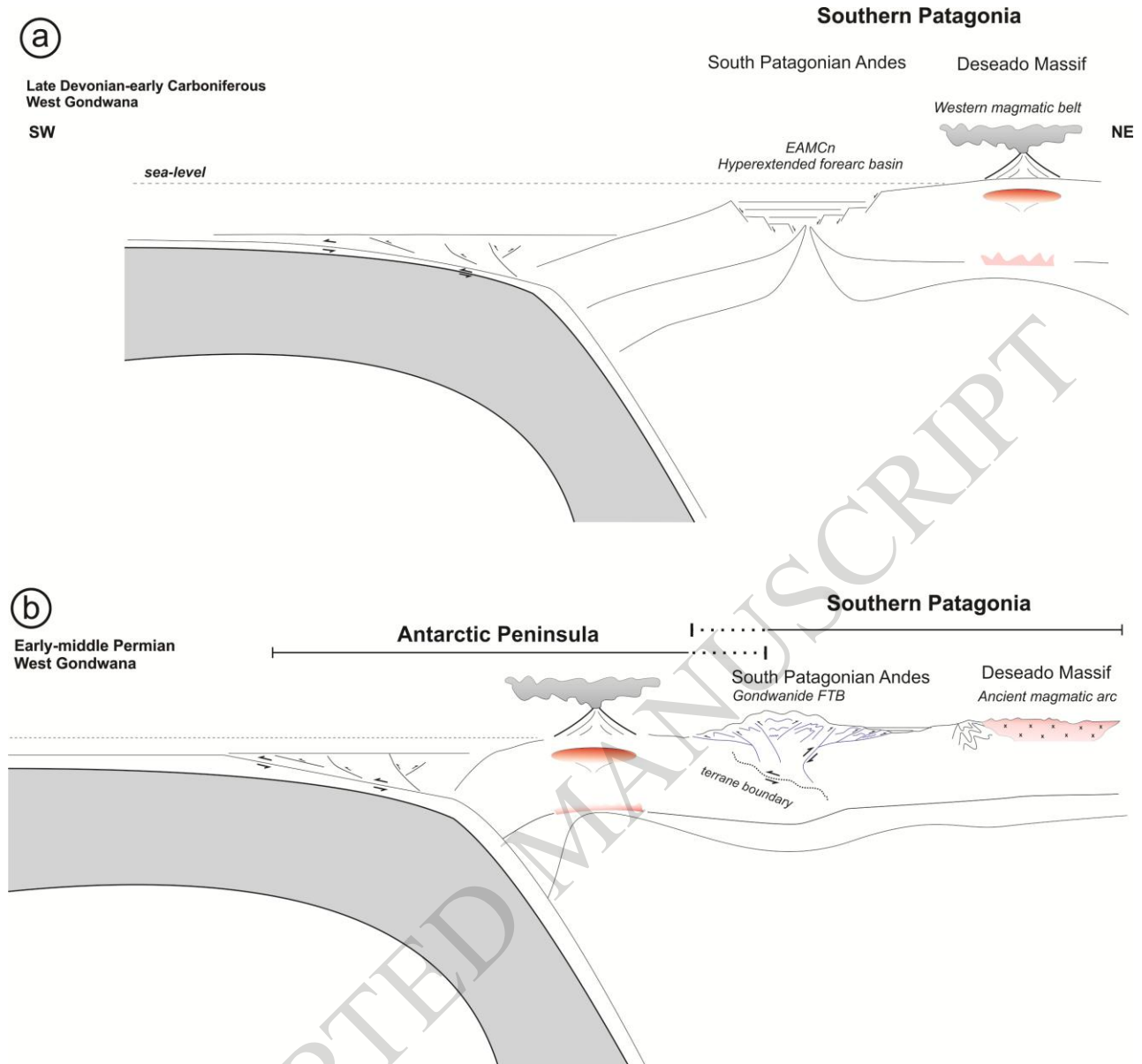


FIGURE 10